

Validity assessment of a single tooth model in clenching and chewing simulations

Yeokyeong Lee^{1,2a}, Minji Kim^{3b}, Ji-Man Park^{4b} and Hee Sun Kim^{*2}

¹Department of Mechanical and Biomedical Engineering, Ewha Womans University,
52 Ewhayeodae-gil, Seodaemun-gu, Seoul 03760, Republic of Korea

²Department of Architectural and Urban Systems Engineering, Ewha Womans University,
52 Ewhayeodae-gil, Seodaemun-gu, Seoul 03760, Republic of Korea

³Department of Orthodontics, College of Medicine, Ewha Womans University, 52 Ewhayeodae-gil,
Seodaemun-gu, Seoul 03760, Republic of Korea

⁴Department of Prosthodontics, Yonsei University College of Dentistry,
50 Yonsei-ro, Seodaemun-gu, Seoul, 03722, Republic of Korea

(Received February 18, 2021, Revised June 25, 2021, Accepted June 28, 2021)

Abstract. Single tooth finite element model is widely used to investigate tooth behaviors with reducing modeling process and computational time. This study aims to examine the validity of a single tooth model in clenching and chewing actions. The single tooth model consisting of tooth #16, the periodontal ligament (PDL), and bone was subjected to coronal-apical movements. The predicted strains from the analyses were validated with the in-vitro experimental results on tooth-PDL-bone specimen. The stress distributions of tooth root and PDL were compared to those from the full skull model to evaluate reasonability of the single tooth model. The results of this study indicate that the single tooth model is able to predict valid structural and mechanical behaviors in clenching and chewing activities.

Keywords: single tooth; validity; clenching; chewing; finite element analysis

1. Introduction

In dentistry and dentofacial orthopedics, finite element (FE) method is a non-invasive tool to simulate biomechanical environments and to resolve problems in clinical tests (Bola *et al.* 2016, Mohamed *et al.* 2018, Nakhli *et al.* 2019, Mobasseri *et al.* 2020, Sallah *et al.* 2020). It is one of critical issues in FE modeling to determine which part is included in the model and can be excluded for the simplification according to the objective and scope of study. Skull models, composed of jawbones and full teeth, are commonly used for the simulation of kinetic loading of jaw system (Bujtar *et al.* 2010, Kim *et al.* 2012, Commisso *et al.* 2015, Choy *et al.* 2017). To evaluate relations of neighboring teeth and bones, multi-teeth model including several teeth and

*Corresponding author, Ph.D. Professor, E-mail: hskim3@ewha.ac.kr

^aPh.D.

^bPh.D. Professor



Fig. 1 The proposed single tooth FE model. Left figure shows a single tooth model consisting of tooth #16, PDL, and bone in blue, orange, and green color, respectively. Right figure shows cross section of the model

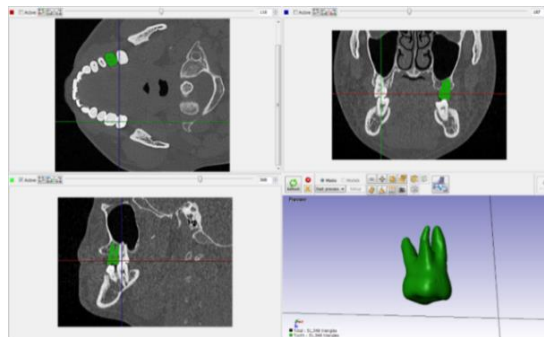


Fig. 2 Construction of the tooth geometry using Scan-IP. From CT scan images of full skull, the geometry of tooth #16 was selected using filtering processes and was obtained as 3D solid model in green color

alveolar bone is proposed (Vicilli *et al.* 2008, Boryor *et al.* 2008, Field *et al.* 2009, Benazzi *et al.* 2011).

Single tooth model is usually used to investigate the mechanical responses under external loading in tooth and periodontal ligament (PDL) levels (Natali *et al.* 2004, Kojima and Fukui 2006, Du *et al.* 2011, Merdji *et al.* 2013). The FE analytical approach focusing on the single tooth behaviors can effectively reduce modeling and computational times compared to cases of multiple teeth and skull models, and help design implant and other prosthodontic devices. Meanwhile, there have been arguments that single tooth model has limitations due to a lack of consideration of the interactions between adjacent teeth. The FE simulations on the single tooth dental implant showed that the maximum stresses and the effects of contact force were affected by the adjacent teeth under the mesial-distal and inclined loadings, especially (Chaichanasiri *et al.* 2009). The comparisons between the FE analyses on single tooth and multi teeth indicated that a multi-teeth system allowed simulating a more real-world biomechanical environment, such as the presence and rigidity of adjacent teeth and bones (Field *et al.* 2009).

Since previously reported researches show both effectiveness and concerns of using single tooth model, it is important to investigate whether stress/strain of tooth can be accurately predictable from the single tooth model under clinical situation. Therefore, this study aimed to validate FE model of a single tooth for the predictions of structural and mechanical behaviors under clenching and chewing conditions. Postulations suggest that the stresses and strains of teeth in the coronal-apical direction are less likely affected by the neighboring teeth and a bone, thus the



(a) Single tooth model with a cap. To simulate clenching activity, a cap part has a groove to be matched with the occlusal surface of the tooth part
 (b) Single tooth model including the food bolus. To simulate chewing, the part of food is generated in rectangular parallelepiped shape

Fig. 3 Single tooth models for clenching and chewing simulations

predictions from a single tooth model can be acceptably reasonable. Towards that goal, the analytical approaches for the clenching and chewing simulations, typical coronal-apical movements of tooth, are proposed with considerations of the tooth, PDL, and bone interactions. The single tooth model is validated by comparisons between the FE analytical results and the in-vitro experimental results to examine accuracy of the proposed modeling method. In addition, the predictions from the single tooth FE model are compared with those from the full skull FE model (Lee *et al.* 2017, Lee *et al.* 2019) to evaluate whether the tooth behaviors can be reasonably predicted from the single tooth model in which the effects of neighboring teeth and bones are not considered.

2. Material and methods

2.1 Development of a single tooth FE model

In this study, an FE model consisting of a tooth, periphery PDL, and simplified alveolar bone was constructed as shown in Fig. 1. The right maxillary first molar (#16) was chosen as the tooth model since it functions as one of the primary teeth for mastication (Martinez Choy *et al.* 2017). Three-dimensional geometry of the tooth was generated using commercial software Scan-IP (Simpleware Ltd, Exeter, United Kingdom) (Fig. 2), and based on computed tomography (CT) scan images of a 38-year-old male skull, the same images used for the full skull models of the existing studies (Lee *et al.* 2017, Lee *et al.* 2019). The tooth model in this study was configured in a curved shape with enough protrusion to construct details of the occlusal surface and dental root. The 3D solid model of the tooth was then imported into commercial software HyperMesh 2017 (Altair, Michigan, United States), a pre-processor for FE modeling, to add the PDL and bone parts, and to refine the meshes. Bone part was simplified as one mass of a cube structure $30 \times 30 \times 30$ mm (width \times length \times height) in size, where the vertical direction (z-direction) was in parallel to the coronal-apical direction of the full skull models. The PDL part was obtained by offsetting the root surface with a uniform distance of 0.2 mm in the positive direction and filling out the interspaces between the root outer surface and the offset surface. Finally, the solid model of the

tooth-PDL-bone complex was meshed using 4-noded tetra element with 1st-order shape function, which has the grading of triangular edge lengths from 0.2 mm to 1.2 mm using Delaunay refinement techniques (Shewchuk 2002, Dechaumphai *et al.* 2003). The single tooth model consisted of 1,721,244 elements: 285,573 for the tooth, 62,108 for the PDL, and 1,373,563 for the bone parts.

As illustrated in Fig. 3(a), a cap part was added for the role of an antagonistic tooth in order to be in contact with the tooth during the clenching simulation. The bottom surface of the cap part was cut into the form of an occlusal surface of the tooth using Boolean operations. The cap part configured in the same negative geometry as the tooth in order to apply clenching force on occlusal surface without causing stress concentration and sliding. In this manner, perfectly matched interfaces between the upper and lower teeth can be simulated which is ideal case during clenching activity from a clinical aspect.

To simulate chewing of food, a part of a food bolus was constructed and located above the single tooth model by covering the occlusal surface of the tooth as shown in Fig. 3(b). The bolus had a rectangular parallelepiped configuration 15 × 23 × 6 mm (width × length × height) in size. Unlike the cap part for the clenching simulation, the food bolus was not cut in the form of the occlusal surface because 1) the food specimens for the experiment were prepared in a cuboid shape without having a groove, and 2) deformation of the food bolus was relatively large so that the contact between the food and the occlusal surface was tightly formed during chewing.

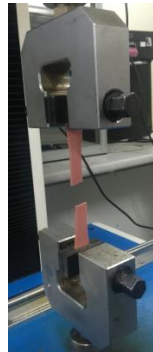
2.2 Material model

In this study, two material cases were considered for the single tooth FE model to validate the single tooth model experimentally and to compare the predictions from full skull models. Material case 1 represented the materials used to fabricate the test specimens, photopolymer resin (Veroclear) and silicone impressions (Examix Fine, GC). According to the given material specifications of photopolymer resin, linear-elastic materials models with an elastic modulus of 2.5 GPa and Poisson's ratio of 0.3 were assigned to the parts of the tooth, bone, and cap. To define the material properties of the silicone impressions, material strength tests were performed as shown in Fig. 4(a). Test specimens were prepared according to ISO 527. Tests were performed to measure elastic modulus and Poisson's ratio of silicone impression according to ASTM D638 and ASTM D695. We found that the stress-strain curve obtained from compressive test was similar to that from tensile test in the initial state. Therefore, elastic modulus for compressive behavior was used to fit the Ramberg-Osgood uniaxial formulation of Eq. (1) as depicted in Fig. 4(b). The fitted formulation and Poisson's ratio of 0.4 (Omori *et al.* 2001) were applied to the PDL part in the form of a nonlinear elastic uniaxial stress-strain constitutive model (Zhao *et al.* 2020).

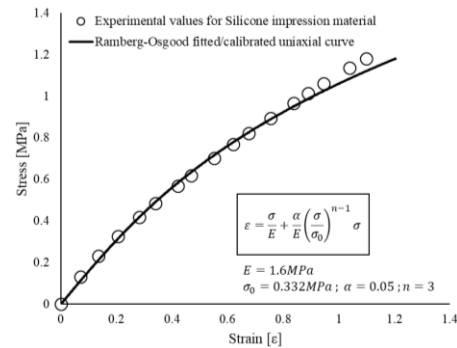
$$\varepsilon = \frac{\sigma}{E} + \frac{\alpha}{E} \left(\frac{\sigma}{\sigma_0} \right)^{n-1} \sigma \quad (1)$$

Where, E=1.6 MPa, $\sigma_0=0.332$ MPa, $\alpha=0.05$, n=3

Material case 2 (Table 1) represented the human tooth, cortical bone, and PDL, to compare the results from the single tooth model with those from full skull models, referring to the existing studies (Lee *et al.* 2017, Lee *et al.* 2019). The full skull models consisted of teeth, skull bones, PDL and TMJ disks, and the skull bones composed of cortical bone and cancellous bone. Bone part in the single tooth model was simplified as one mass of cortical bone since the scope of this



(a) Material strength test



(b) Ramberg-Osgood uniaxial curve fitting

Fig. 4 Material model for the PDL part in material case 1 (silicone impression)

Table 1 Material properties of the human tooth, cortical bone, and PDL (material case 2)

Part	Material properties		Reference
	Elastic modulus	Poisson's ratio	
Human tooth	20.0 GPa	0.30	Mahoney <i>et al.</i> 2000, Kinney <i>et al.</i> 2003, Ryou <i>et al.</i> 2001, Merdji <i>et al.</i> 2013
Cortical bone	14.5 GPa	0.32	Merdji <i>et al.</i> 2013
PDL	7.5×10^{-4} GPa	0.45	Middleton <i>et al.</i> 1996, Motoyoshi <i>et al.</i> 2002

study was to investigate mechanical behaviors of tooth and PDL, not bone. Regarding the material properties of the human tooth, this study used linear elastic and non-composite material properties of dentin (Mahoney *et al.* 2000, Kinney *et al.* 2003, Ryou *et al.* 2011, Merdji *et al.* 2013). De Santis *et al.* (2002) reported that the slopes of the stress-strain curves for the tooth structures were almost linear, which have been widely adopted for FE models of teeth in the existing literatures. Cortical bone materials used elastic modulus and Poisson's ratio derived from the study by Merdji *et al.* (2013). In addition, the linear-elastic models of the PDL part were assumed as proposed by Middleton *et al.* (1996) and Motoyoshi *et al.* (2002). Although PDL material behavior is more complicated than tooth and bone, most previous studies on the structural behaviors under short-term forces, i.e., clenching and chewing forces, have assumed that the PDL exhibits linear-elastic stress/strain behaviors (Kojima and Fukui 2006, Vecilli *et al.* 2008, Field *et al.* 2009, Poiate *et al.* 2009, Panagiotopoulou *et al.* 2011).

In the chewing simulation, hard candy (Cough drop, Lotte, Korea) was chosen as the material for the food bolus to show tooth behaviors under short-term loading condition. Since the candy has relatively high elasticity and brittleness, the effect of time dependent material behaviors can be neglected from the analyses. To define the material characteristics of the candy, material strength tests were conducted with the specimen prepared in similar sizes to the FE food model, $15 \times 23 \times 6$ mm (width \times length \times height), using a universal testing machine. According to the test results, the linear-elastic material models of candy ($E=120.17$ MPa, $\nu=0.2$) was assigned to the food bolus part. To show tooth behaviors in chewing simulations with different food materials, raw carrot and beef jerky were used for parametric study. The material properties of carrot ($E=7.34$ MPa, $\nu=0.3$) and jerky (hyper-elastic material model proposed by Ogden; $N=1$, $\mu_1=0.1$, $\alpha_1=0.9$, $D_1=9.2$) were also defined according to the same test method as described above for candy.



(a) Tooth specimen applied with the silicone impression for the PDL (b) Tooth installed into the bone cube (c) Test setup. The bone cube was clamped to test-zig

Fig. 5 Specimen preparation and test setup

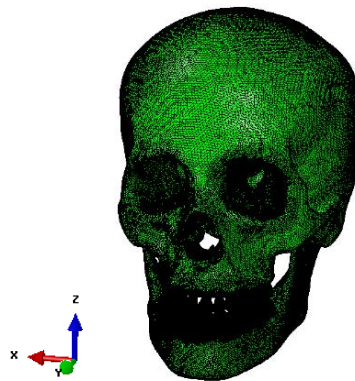


Fig. 6 Full skull FE model for validation (Lee *et al.* 2017, Lee *et al.* 2019)

2.3 Clenching and chewing simulations

Clenching and chewing were simulated by moving the cap and food bolus parts downward 5 mm in the form of displacement control, respectively. The contact issues were resolved using a contact formulation with the assumption of the tooth defined as the master, and the cap or food bolus as slave surfaces. In addition, finite sliding contact with a friction coefficient of 0.2 (Zheng *et al.* 2003, Wierszycki *et al.* 2006) was used for the contact behaviors between the tooth and food bolus. For boundary conditions, the nodes at the bottom surface of bone were constrained in all translational directions. Geometrical nonlinearity and automatic control of the time increment were considered during the analyses. For effective calculation, maximum and minimum time increments (Abaqus analysis user's manual) were set as 0.01 second and 1×10^{-5} seconds, respectively.

2.4 Validation methods

This section describes two cases of validation methods for the proposed single tooth FE model. First method is to validate with the experimental approach. Based on the geometry of the FE model of the single tooth, test specimens consisting of a tooth, bone cube, and cap were fabricated with photopolymer resin (Veroclear, $E=2.5$ GPa, $\nu=0.3$). To generate the PDL, silicone impression (Examix Fine, GC, $E=1.6$ MPa, $\nu=0.4$) was thinly applied to the roots as shown in Fig. 5(a). Strain



Fig. 7 Alphabetical representation of the roots. The roots in the palatal, mesial, and distal aspects are represented by A, B, and C, respectively. Root C is the smallest radicular root among the three

gauges (FLA-03-11-1L, TML, gauge length=0.3 mm) were attached to the outer surface of each root before the application of the silicone impression. The tooth was then installed into the bone cube (Fig. 5(b)), and the specimen was placed between the loading plate and clamp of the loading machine as illustrated in Fig. 5(c). Finally, the specimen was subjected to axial loading of 300N, which is the maximum bite force at the first molar (Helkimo *et al.* 1977, Sultana *et al.* 2002, Sonnesen and Bakke 2005). The loading was repeated five times to ensure consistency of the test results. Strains of the roots were acquired using a data logger (TDS-303, Tokyo Measuring Instruments Laboratory Co., Ltd., Japan) with a frequency of 50Hz. Moreover, the in-vitro experiments were repeated with the addition of the food bolus to simulate chewing of food, such that the food bolus of hard candy (Cough drop, Lotte) was prepared at the size of $15 \times 23 \times 6$ mm (width \times length \times height) and placed between the tooth specimen and loading plate.

Second validation method is to compare with the predicted stress from FE analyses on the full skull model (Fig. 6). The full skull modeling process has been proposed and validated experimentally in the previous studies (Lee *et al.* 2017, Lee *et al.* 2019). Both full skull model and single tooth model use material characteristics of the human tooth, PDL, and bone (material case 2) for predicting realistic stress distributions of the tooth and PDL. In the full skull model of the clenching simulation, a z-directional force of 300N was evenly distributed to the occlusal surface of tooth #16 in order to obtain the same loading conditions seen in the single tooth model. For the chewing simulation, the hard candy bolus in the full skull model was moved upward 5 mm in the form of displacement control.

3. Result

3.1 Comparison between experiment and FE analysis of single tooth model

The first assessment involved the strains from the experiments and the FE analyses of the single tooth model applying material case 1. The predicted strains from FE analyses were obtained by averaging the z-directional strains of the elements where strain gauges were located in the experiments. The tooth roots in the palatal, mesial, and distal aspects are represented by A, B, and C, respectively (Fig. 7).

In clenching simulations (Fig. 8(a)) when maximum load of 300N, the experimental strains (Exp) at roots A, B, and C were measured as -7,238, -1,123, and 1,240 $\mu\epsilon$, respectively. From the FE analysis, strains (FEA) at roots A, B, and C were predicted as -6,629, -1,207, and 957 $\mu\epsilon$,

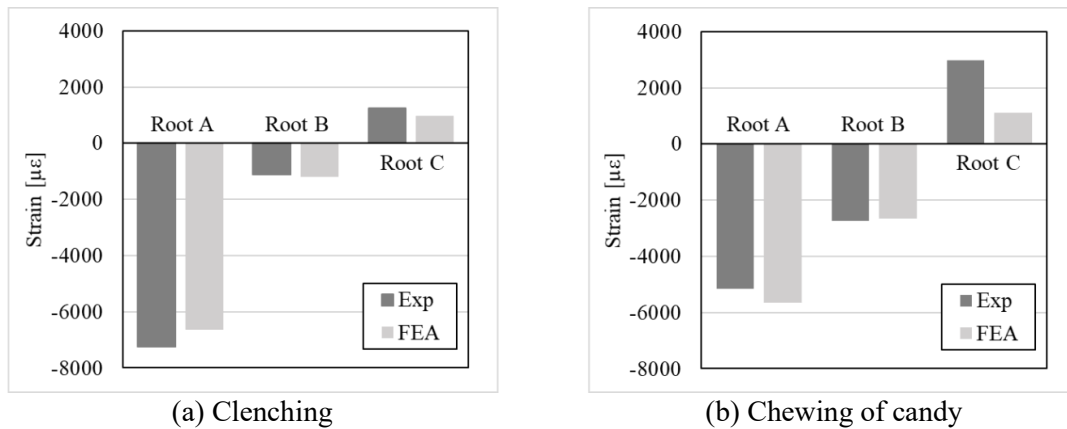


Fig. 8 Strains of tooth roots A, B, and C at maximum load of 300N from the experiment and FE analysis of the single tooth model. Both experimental (Exp: dark grey) and analytical (FEA: light grey) results were well agreed to each other under clenching and chewing simulations

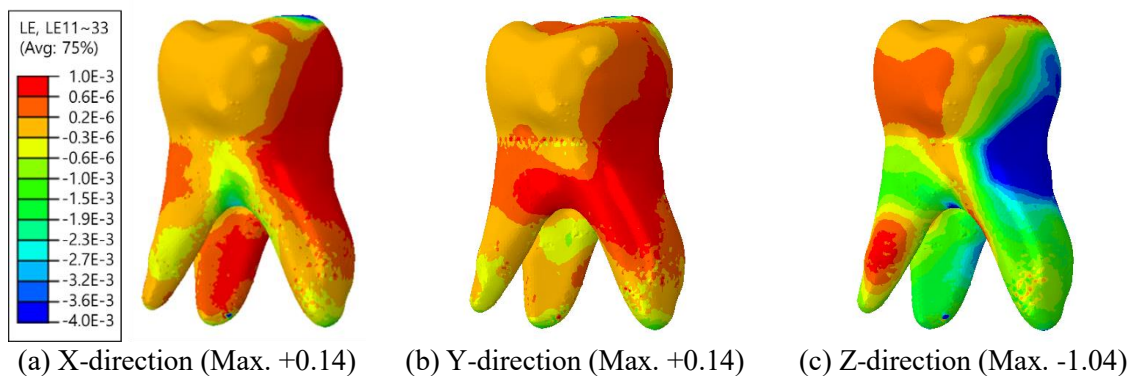


Fig. 9 Logarithmic strain distributions of the single tooth model

respectively. In chewing of the candy (Fig. 8(b)), the experimental strains (Exp) at roots A, B, and C were $-5,169$, $-2,742$, and $2,981 \mu\epsilon$, respectively. The predicted strains from FE analysis (FEA) at roots A, B, and C were $-5,645$, $-2,646$, and $1,107 \mu\epsilon$, respectively. The differences between the experimental and the FE predicted strain values were 3.5–9.2%, except for the results from root C. In root C, relatively large discrepancies between the experiment and the prediction were observed, such that the predicted strains were smaller than the experimental results.

This section focuses on the z-directional strains, because the z-direction is matched with the directions of clenching as well as chewing. Moreover, strains in the x- and y-directions were much lower than that in the z-direction as shown in Fig. 9. The maximum strain value in the z-direction was obtained from the single tooth model as $1.04 \mu\epsilon$ in compression, while those in the x- and y-directions were approximately $0.14 \mu\epsilon$ in tension.

3.2 Comparison between FE analyses of full skull model and single tooth model

The second assessment involved the predictions from full skull FE models and single tooth FE

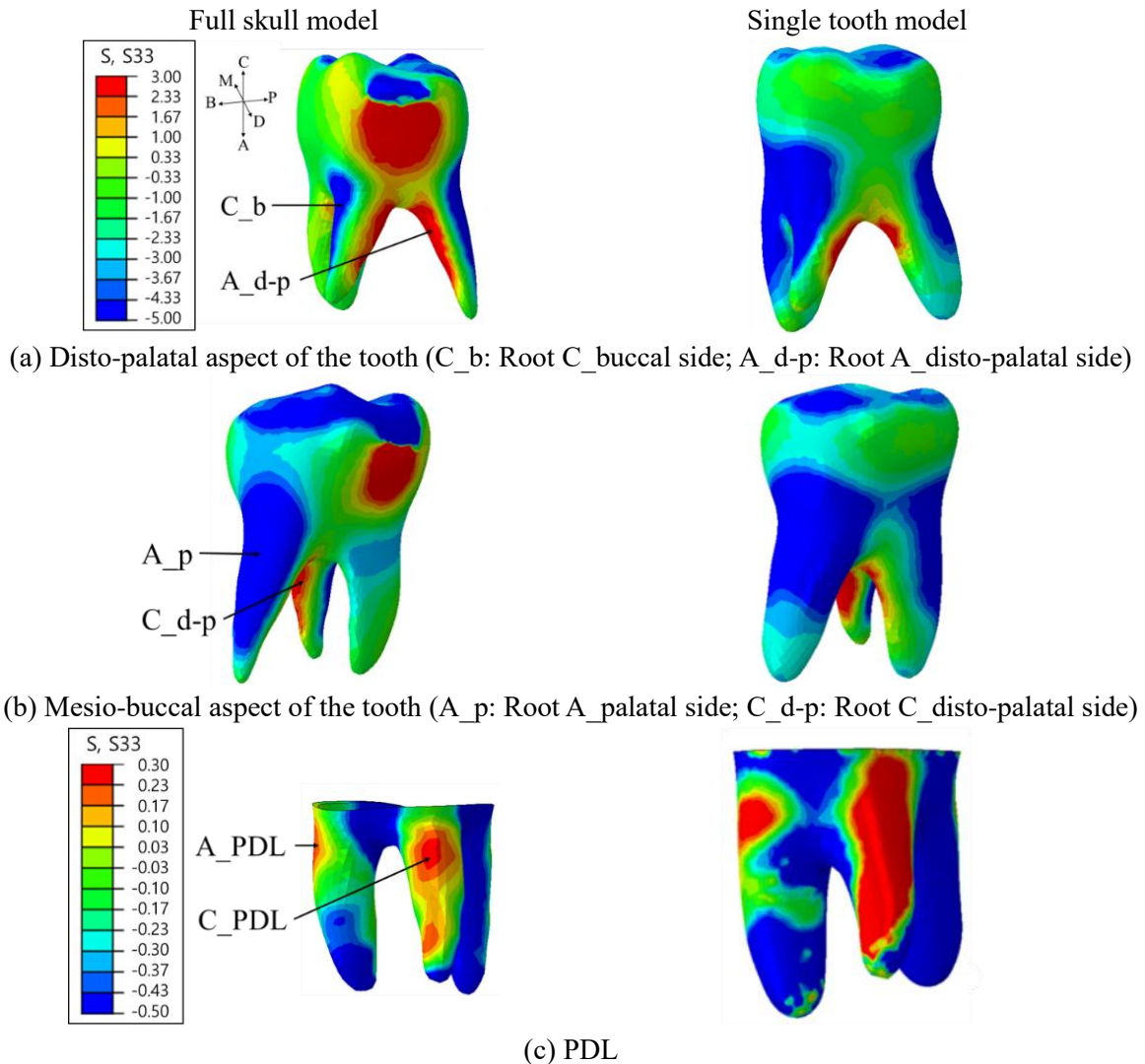


Fig. 10 The z-directional stress distributions of tooth #16 and PDL #16 in the full skull model (left column) and the single tooth model (right column) under clenching simulations at force level of 300N (unit : MPa)

models. Fig. 9 shows the z-directional stress distributions of tooth #16 and the PDL of #16 under clenching simulations at a bite force level of 300N. Overall, the stress distributions were similar in both models, such that relatively high tensile stresses were observed in the disto-palatal aspects of roots A and C, whereas the palatal side of root A and the buccal side of root C exhibited compressive stresses (Figs. 10(a) and (b)). As shown in Fig. 10(c), high tensile stresses at PDL were observed in the apex of roots A and C.

From the chewing simulations at a force level of 100N, the z-directional stress distributions of tooth #16 and PDL of #16 were obtained as illustrated in Fig. 9. In detail, both models predicted high tensile stresses at the disto-palatal aspects of roots A and C. High compressive stresses were

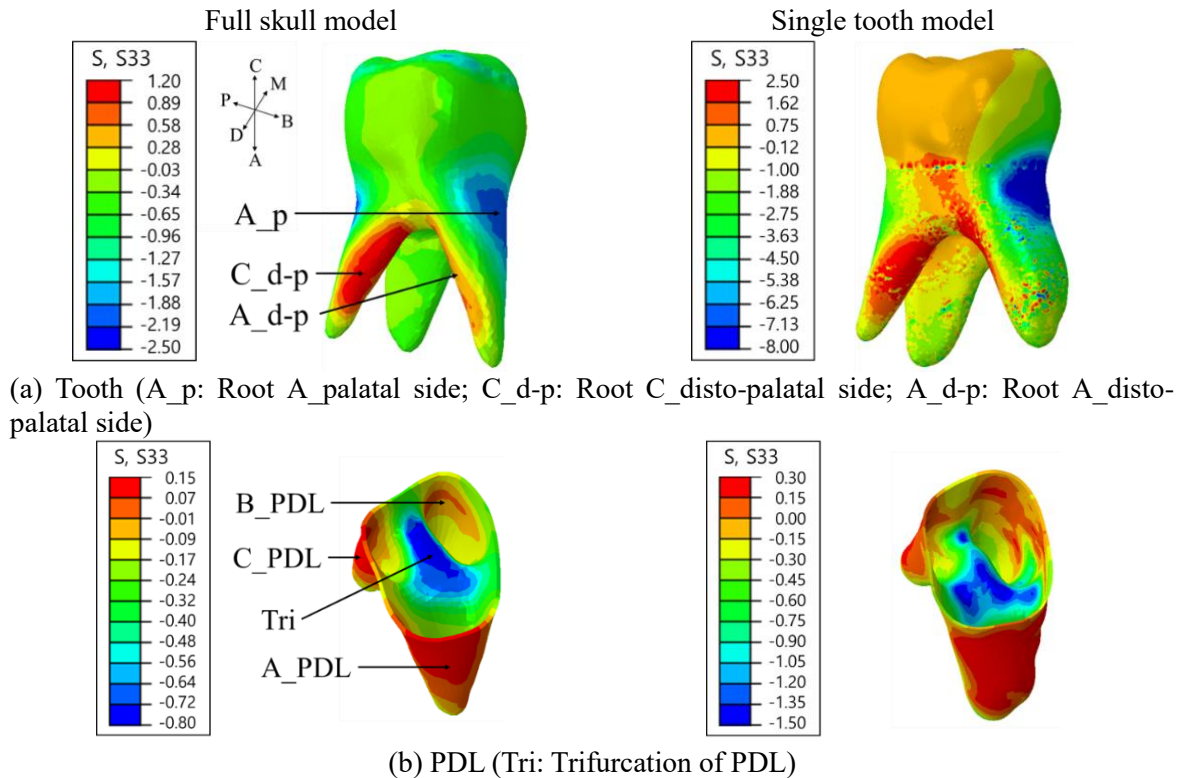


Fig. 11 The z-directional stress distributions of tooth #16 and PDL #16 in the full skull model (left column) and the single tooth model (right column) under chewing simulations at force level of 100N. Note that different scales of stress legends are used depending on the models and parts. (unit : MPa)

observed from the palatal side of root A, especially on the cemento-enamel junction (Fig. 11(a)). Fig. 11(b) also shows similar stress distributions of the PDL in the full skull model and single tooth model, such that the tensile stresses were concentrated at the apex of the three roots, while stresses at the bottom of the trifurcation were in compression. Stresses at each region predicted from the FE simulations on the full skull model and the single tooth model were tabulated in Table 2.

3.3 Comparison between chewing simulations of single tooth model with different foods

In this section, tooth behaviors in chewing simulations were compared according to different food materials. Fig. 12 depicts the relationships between displacement of food bolus and reaction force at the fixed region of the single tooth models depending on candy, carrot and jerky. The slopes of the curves and the forces predicted at the same displacement are the largest in the case of candy, followed by carrot and jerky. It is interesting to note that the stiffest stress-strain curve is also found from candy, where the lowest slope is for the jerky as shown in Fig. 13.

The slope of force-displacement curve from the case of candy is approximately 1.8 times higher than that of carrot although elastic modulus of candy (120.7MPa) is around 16 times larger

Table 2 The z-directional stresses predicted from the FE analyses on the full skull model and the single tooth model

Simulation	Model	Region	Stress [MPa]	Related figure
Clenching	Full skull	C_b	-7.824	Fig. 8(a)
		A_d-p	4.722	
		A_p	-10.586	Fig. 8(b)
		C_d-p	3.698	
		A_PDL	0.261	Fig. 8(c)
		C_PDL	0.298	
	Single tooth	C_b	-7.246	Fig. 8(a)
		A_d-p	4.388	
		A_p	-11.310	Fig. 8(b)
		C_d-p	3.932	
		A_PDL	0.271	Fig. 8(c)
		C_PDL	0.366	
Chewing	Full skull	A_p	-2.389	Fig. 9(a)
		C-d-p	1.470	
		A_d-p	1.365	Fig. 9(b)
		B_PDL	0.043	
		C_PDL	0.137	Fig. 9(b)
		Tri	-0.785	
	Single tooth	A_PDL	0.159	Fig. 9(a)
		A_p	-7.421	
		C-d-p	3.301	Fig. 9(b)
		A_d-p	3.956	
		B_PDL	0.081	Fig. 9(b)
		C_PDL	0.150	
Tri	-0.822	Fig. 9(b)		
A_PDL	0.467			

C_b: Buccal side of root C; A_d-p: Disto-palatal side of root A; A_p: Palatal side of root A; C_d-p: Disto-palatal side of root C; A_PDL: PDL of root A; C_PDL: PDL of root C; B_PDL: PDL of root B; Tri: Trifurcation at PDL

than that of carrot (7.34MPa). It is predicted that bite force during chewing of harder and stiffer food increases, but this increased amount is not proportional to the discrepancy among material properties of food.

4. Discussions

Both the experiment and FE analysis on the single tooth model show that roots A and B

underwent compressive strains, while root C exhibited tensile strains (Fig. 8). It is most likely that the dental roots were compressed as the tooth was subjected to clenching and chewing forces. However, root C was in tension maybe because root C is the smallest radicular root among the three and it an outstretched shape unlike the other roots. This particular shape of root C might cause leaning of the tooth as other roots were forced toward the bottom. Moreover, the predicted strains from FE analyses were lower than the experimental strains, especially in root C. This may be due to the differences in the geometries of the test specimen and the FE model. In preparation of the test specimen, the circumstantial bone of the root had to be relatively large in order to make the insertion of the tooth easier. In addition, the silicone impression material was not evenly applied to the roots, which stiffened the experimental strain-force curves. Geometrical sensitivity could also be found in the existing literature, where Hohmann *et al.* (2011) reported that geometry is a critical factor in determining the structural behaviors of a tooth applied with high loads, such as bite forces in our FE studies. The studies conducted by Choy *et al.* (2000) and Ona and Wakabayashi (2006) suggested that the reduction of alveolar bone height and the widening of the PDL space creates an increase in maximum principal stress in the periodontal structures. In addition, PDL thickness has a remarkable effect on stress distributions in the tooth and PDL (Hohmann *et al.* 2011, Vikram *et al.* 2012). From both the clenching and chewing simulations, the predicted strains from FE analyses were well-matched with those of the experiment, except for root C. This result indicates that the surrounding PDL and bone were relatively sensitive to geometry due to root C being the smallest among the three roots. Considering the geometrical differences, it can be justified that the accuracy of the proposed single tooth model is valid experimentally in clenching and chewing simulations.

In comparison between the FE models of full skull and single tooth, the bone part in the single tooth model is simplified as one mass of cortical bone, while the full skull model is composed with cortical bone and cancellous bone. Despite of the simplification of the bone part in the single tooth model, stress distributions of the root and PDL were comparable to those predicted from the full skull model. The study conducted by Nevah *et al.* (2012) also reported that the overall tooth movement responses were similar regardless of the materials where tooth was embedded, through the in-vitro experiments on tooth in the mandible and the tooth in Epoxy. However, adjacent teeth in the full skull FE model cause the differences of stress contour at crown. From the clenching simulations, the tooth in the full skull model exhibited high tensile stresses at the mesial and distal aspects of the crown (Figs. 10(a) and 10(b)) due to the contact forces between tooth #16 and the adjacent teeth (#15 and #17). As illustrated in Fig. 11(a), the crown of the single tooth model experienced relatively higher stresses than the full skull model with stress ranges in both models being different under chewing simulations. This is due to the interfaces between the tooth and food bolus being not modeled as a perfect match in the single tooth model, while the food bolus in the full skull model was cut in the form of the occlusal surfaces of the antagonistic teeth. Nonetheless, the degrees of discrepancy in the crown can be neglected, because the stresses observed in the crown were much smaller than those in the root and crown is not important part to evaluate tooth behaviors in coronal-apical direction. It is reported that the short-term structural behavior of teeth is primarily governed by their PDL because teeth are virtually rigid and are connected to an almost as rigid alveolar bone by the PDL (Natali 2003). Since our clenching and chewing simulations can be considered as a short-term tooth movement in coronal-apical direction, the PDL and the root covered by the PDL are more important regions to evaluate the structural behaviors of tooth. In considering the stress distributions of the root and PDL, the proposed single tooth model is in good agreement with the full skull model under clenching and chewing simulations. It intends that the

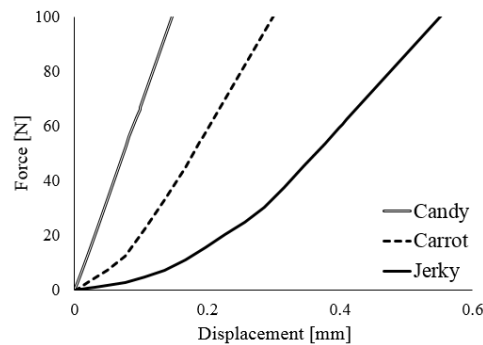


Fig. 12 Force-displacement curves from chewing simulations with different foods

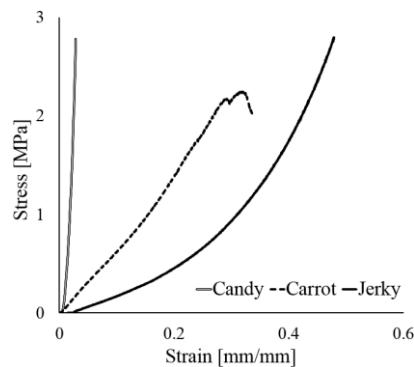


Fig. 13 Stress-strain curves of food materials obtained from tests

single tooth FE model is a reasonable approach to simulate and predict the tooth behaviors in the coronal-apical direction.

Even though the modeling methods were validated in short-term movement, the single tooth model might overestimate structural and mechanical behaviors when simulating large deformation or long-term movement. It is because this study used the simplified material properties, boundary conditions, and contact formulations based on the assumptions. If the observation of the behaviors in large deformation and long-term movement is required, the limitations must be overcome using micro-level composite material models and applying contact formulations between junctions. Nevertheless, the proposed single tooth model is justified since the scope of this study considered only small deformation of parts and short-term movements of clenching and chewing.

5. Conclusions

This study presents the single tooth model for predicting tooth behaviors under clenching and chewing simulations.

- The accuracy of the proposed single tooth FE model is validated with the in-vitro test using tooth-PDL-bone complex. The strains of tooth roots obtained from FE analysis are in good agreement with the experimental results in general. The discrepancy can be explained by the geometrical differences between the FE model and the test specimen.

- The comparison with the full skull FE model shows that the tooth behaviors in coronal-apical direction are reasonably predictable from the single tooth model. It intends that the predictions from the single tooth model are acceptably reasonable though the effects of neighboring teeth and bone are not considered.
- The proposed single tooth model is able to predict structural and mechanical behaviors of tooth-PDL-bone complex under clenching and chewing conditions.

Acknowledgments

The research was supported by Basic Science Research Program through the National Research Foundation of Korea (NRF) funded by the Ministry of Education (NRF-2018R1D1A1A2085366).

References

- ABAQUS Documentation (2013), *Abaqus Analysis User's Manual*, Dassault Systèmes, Troy, MI, U.S.A.
- Benazzi, S., Kullmer, O., Grosse, I.R. and Weber, G.W. (2011), "Using occlusal wear information and finite element analysis to investigate stress distributions in human molars", *J. Anat.*, **219**(3), 259-272. <https://doi.org/10.1111/j.1469-7580.2011.01396.x>.
- Bola, A.M., Ramos, A. and Simoes, J.A. (2016), "Sensitivity analysis for finite element modeling of humeral bone and cartilage", *Biomat. Biomech. Bioeng.*, **3**(2), 71-84. <http://dx.doi.org/10.12989/bme.2016.3.2.071>.
- Boryor, A., Geiger, M., Hohmann, A., Wunderlich, A., Sander, C., Sander, F.M. and Sander, F.G. (2008), "Stress distribution and displacement analysis during an intermaxillary disjunction – a three-dimensional FEM study of a human skull", *J. Biomech.*, **41**(2), 376-382. <https://doi.org/10.1016/j.jbiomech.2007.08.016>.
- Bujtar, P., Sandor, G.K., Bojtos, A., Szucs, A. and Barabas, J. (2010), "Finite element analysis of the human mandible at 3 different stages of life", *Oral Surg., Oral Med., Oral Pathol., Oral Radiol., Endodontol.*, **110**(3), 301-309. <https://doi.org/10.1016/j.tripleo.2010.01.025>.
- Chaichanasiri, E., Nanakorn, P., Tharanon, W. and Vander Sloten, J. (2009), "A finite element study of the effect of contact forces between an implant-retained crown and its adjacent teeth on bone stresses", *J. Mech.*, **25**(4), 441-450. <https://doi.org/10.1017/S1727719100002926>.
- Choy, K., Pae, E.K., Park, Y., Kim, K.H. and Burstone, C.J. (2000), "Effect of root and bone morphology on the stress distribution in the periodontal ligament", *Am. J. Orthod. Dentofac. Orthop.*, **117**(1), 98-105. [https://doi.org/10.1016/S0889-5406\(00\)70254-X](https://doi.org/10.1016/S0889-5406(00)70254-X).
- Choy, S.E.M., Lenz, J., Schweizerhof, K., Schmitter, M. and Schindler, H.J. (2017), "Realistic kinetic loading of the jaw system during single chewing cycles: a finite element study", *J. Oral Rehabil.*, **44**(5), 375-384. <https://doi.org/10.1111/joor.12501>.
- Commisso, M.S., Martinez-Reina, J., Ojeda, J. and Mayo, J. (2015), "Finite element analysis of the human mastication cycle", *J. Mech. Behav. Biomed. Mater.*, **41**, 23-35. <https://doi.org/10.1016/j.jmbbm.2014.09.022>.
- De Santis, R., Ambrosio, L. and Nicolais, L. (2002), *Mechanical Properties of Tooth Structures*, In: *Integrated Biomaterials Science*, Springer, Boston, MA, USA.
- Dechaumphai, P., Phongthanapanich, S. and Bhandhubanyong, P. (2003), "Adaptive finite elements by Delaunay triangulation for fracture analysis of cracks", *Struct. Eng. Mech.*, **15**(5), 563-578. <http://dx.doi.org/10.12989/sem.2003.15.5.563>.
- Du, J.K., Lin, W.K., Wang, C.H., Lee, H.E., Li, H.Y. and Wu, J.H. (2011), "FEM analysis of the mandibular first premolar with different post diameters", *Odontol.*, **99**(2), 148-154. <https://doi.org/10.1007/s10266-011-0011-8>.

- El Sallah, Z.M., Ali, B. and Abderahmen, S. (2020), "Effect of force during strumbling of the femur fracture with a different ce-mented total hip prosthesis", *Biomat. Biomech. Bioeng.*, **5**(1), 11-23. <https://doi.org/10.12989/bme.2020.5.1.011>.
- Field, C., Ichim, I., Swain, M.V., Chan, E., Darendeliler, M.A., Li, W. and Li, Q. (2009), "Mechanical responses to orthodontic loading: a 3-dimensional finite element multi-tooth model", *Am. J. Orthod. Dentofac. Orthop.*, **135**(2), 174-181. <https://doi.org/10.1016/j.ajodo.2007.03.032>.
- Helkimo, E., Carlsson, G.E. and Helkimo, M. (1977), "Bite force and state of dentition", *Acta. Odontol. Scand.*, **35**(6), 297-303. <https://doi.org/10.3109/00016357709064128>.
- Hohmann, A., Kober, C., Young, P., Dorow, C., Geiger, M., Boryor, A., Sander, F.M., Sander, C. and Sander, F.G. (2011), "Influence of different modeling strategies for the periodontal ligament on finite element simulation results", *Am. J. Orthod. Dentofac. Orthop.*, **139**(60), 775-783. <https://doi.org/10.1016/j.ajodo.2009.11.014>.
- Kim, H.S., Park, J.Y., Kim, N.E., Shin, Y.S., Park, J.M. and Chun, Y.S. (2012), "Finite element modeling technique for predicting mechanical behaviors on mandible bone during mastication", *J. Adv. Prosthod.*, **4**(4), 218-226. <http://dx.doi.org/10.4047/jap.2012.4.4.218>.
- Kinney, J.H., Habelitz, S., Marshall, S.J. and Marshall, G.W. (2003), "The importance of intrafibrillar mineralization of collagen on the mechanical properties of dentin", *J. Dent. Res.*, **82**(12), 957-961. <https://doi.org/10.1177/154405910308201204>.
- Kojima, Y. and Fukui, H. (2006), "A numerical simulation of tooth movement by wire bending", *Am. J. Orthod. Dentofac. Orthop.*, **130**(4), 452-459. <https://doi.org/10.1016/j.ajodo.2005.01.028>.
- Lee, Y.K. and Chun, Y.S. (2020), "An investigation into structural behaviors of skulls chewing food in different occlusal relationships using FEM", *Clin. Exp. Dent. Res.*, **6**(3), 277-285. <https://doi.org/10.1002/cre2.273>.
- Lee, Y.K., Kim, H.S. and Park, J.Y. (2017), "The case study of masticatory force with food from full skull and partial model", *Int. J. Precis. Eng. Manuf.*, **18**(10), 1455-1462. <https://doi.org/10.1007/s12541-017-0173-6>.
- Mahoney, E., Holt, A., Swain, M. and Kilpatrick, N. (2000), "The hardness and modulus of elasticity of primary molar teeth: an ultra-micro-indentation study", *J. Dent.*, **28**(8), 589-594. [https://doi.org/10.1016/S0300-5712\(00\)00043-9](https://doi.org/10.1016/S0300-5712(00)00043-9).
- Martinez Choy, S.E., Lenz, J., Schweizerhof, K., Schmitter, M. and Schindler, H.J. (2017), "Realistic kinetic loading of the jaw system during single chewing cycles: a finite element study", *J. Oral Rehabil.*, **44**(5), 375-384. <https://doi.org/10.1111/joor.12501>.
- Merdji, A., Mootanah, R., Bouiadjra, B.A.B., Benaissa, A., Aminallah, L. and Mukdadi, S. (2013), "Stress analysis in single molar tooth", *Mater. Sci. Eng. Civil*, **33**(2), 691-698. <https://doi.org/10.1016/j.msec.2012.10.020>.
- Middleton, J., Jones, M. and Wilson, A. (1996), "The role of the periodontal ligament in bone modeling: the initial development of a time-dependent finite element model", *Am. J. Orthod. Dentofac. Orthop.*, **109**(2), 155-162. [https://doi.org/10.1016/S0889-5406\(96\)70176-2](https://doi.org/10.1016/S0889-5406(96)70176-2).
- Mobasseri, S., Sadeghi, M., Janghorban, M. and Tounsi, A. (2020), "Approximated 3D non-homogeneous model for the buckling and vibration analysis of femur bone with femoral defects", *Biomat. Biomech. Bioeng.*, **5**(1), 25-35. <https://doi.org/10.12989/bme.2020.5.1.025>.
- Mohamed, C., Abderahmane, S. and Benbarek, S. (2018), "Fracture behavior modeling of a 3D crack emanated from bony inclusion in the cement PMMA of total hip replacement", *Struct. Eng. Mech.*, **66**(1), 37-43. <https://doi.org/10.12989/sem.2018.66.1.037>.
- Motoyoshi, M., Hirabayashi, M., Shimazaki, T. and Namura, S. (2002), "An experimental study on mandibular expansion: increases in arch width and perimeter", *Eur. J. Orthod.*, **24**(2), 125-130. <https://doi.org/10.1093/ejo/24.2.125>.
- Nakhli, Z., Hatira, F.B., Pithioux, M., Chabrand, P. and Saanouni, K. (2019), "Femoral Fracture load and damage localization pattern prediction based on a quasi-brittle law", *Struct. Eng. Mech.*, **72**(1), 000-000. <https://doi.org/10.12989/sem.2019.72.1.000>.
- Natali, A.N. (2003), *Dental Biomechanics*, Taylor & Francis, CRC Press, London, U.K.

- Natali, A.N., Pavan, P.G. and Scarpa, C. (2004), "Numerical analysis of tooth mobility: formulation of a non-linear constitutive law for the periodontal ligament", *Dent. Mater.*, **20**(7), 623-629. <https://doi.org/10.1016/j.dental.2003.08.003>.
- Nevah, G.S.R., Chattah, N.L.T., Zaslansky, P., Shahar, R. and Weiner, S. (2012), "Tooth-PDL-bone complex: Response to compressive loads encountered during mastication – A reviews", *Arch. Oral Biol.*, **57**(12), 1575-1584. <https://doi.org/10.1016/j.archoralbio.2012.07.006>.
- Omori, K., Arikawa, H. and Inoue, K. (2001), "An evaluation of elastomeric impression materials based on surface compressive strength", *J. Oral Rehabil.*, **28**(4), 320-327. <https://doi.org/10.1046/j.1365-2842.2001.00660.x>.
- Ona, M. and Wakabayashi, N. (2006), "Influence of alveolar support on stress in periodontal structures", *J. Dental Res.*, **85**(12), 1087-1091. <https://doi.org/10.1177/154405910608501204>.
- Panagiotopoulou, O., Kupczik, K. and Cobb, S.N. (2011), "The mechanical function of the periodontal ligament in the macaque mandible: a validation and sensitivity study using finite element analysis", *J. Anat.*, **218**(1), 75-86. <https://doi.org/10.1111/j.1469-7580.2010.01257.x>.
- Poiate, I.A.V.P., de Vasconcellos, A.B., de Santana, R.B. and Poiate, Jr E. (2009), "Three-dimensional stress distribution in the human periodontal ligament in masticatory, parafunctional, and trauma loads: finite element analysis", *J. Periodontol.*, **80**(11), 1859-1867. <https://doi.org/10.1902/jop.2009.090220>.
- Ryou, H., Niu, L.N., Dai, L., Pucci, C.R., Arola, D.D., Pashley, D.H. and Tay, F.R. (2011), "Effect of biomimetic remineralization on the dynamic nanomechanical properties of dentin hybrid layers", *J. Dent. Res.*, **90**(9), 1122-1128. <https://doi.org/10.1177/0022034511414059>.
- Shewchuk, J.R. (2002), "Delaunay refinement algorithms for triangular mesh generation", *Comput. Geom.*, **22**(1-3), 21-74. [https://doi.org/10.1016/S0925-7721\(01\)00047-5](https://doi.org/10.1016/S0925-7721(01)00047-5).
- Somesen, L. and Bakke, M. (2005), "Molar bite force in relation to occlusion, craniofacial dimensions, and head posture in pre-orthodontic children", *Eur. J. Orthod.*, **27**(1), 58-63. <https://doi.org/10.1093/ejo/cjh069>.
- Sultana, M.H., Yamada, K. and Hanada, K. (2002), "Changes in occlusal force and occlusal contact area after active orthodontic treatment: a pilot study using pressure-sensitive sheets", *J. Oral Rehabil.*, **29**(5), 484-491. <https://doi.org/10.1046/j.1365-2842.2002.00849.x>.
- Viecilli, R.F., Katona, T.R., Chen, J., Hartsfield, Jr J.K. and Roberts, W.E. (2008), "Three-dimensional mechanical environment of orthodontic tooth movement and root resorption", *Am. J. Orthod. Dentofac. Orthop.*, **133**(6), 791-e11. <https://doi.org/10.1016/j.ajodo.2007.11.023>.
- Vikram, N.R., Kumar, K.S., Nagachandran, K.S. and Hashir, Y.M. (2012), "Apical stress distribution on maxillary central incisor during various orthodontic tooth movements by varying cemental and two different periodontal ligament thicknesses: a FEM study", *Indian J. Dent. Res.*, **23**(2), 213-220. <https://doi.org/10.4103/0970-9290.100429>.
- Wierszycki, M., Kąkol, W. and Łodygowski, T. (2006), "The screw loosening and fatigue analyses of three dimensional dental implant model", *2006 ABAQUS Users' Conference* (Vol. 15), Providence, RI, U.S.A, May.
- Zhao, B., Hu, J., Chen, W., Chen, J. and Jing, Z. (2020), "A nonlinear uniaxial stress-strain constitutive model for viscoelastic membrane materials", *Polym. Test.*, **90**, 106633. <https://doi.org/10.1016/j.polymertesting.2020.106633>.
- Zheng, J., Zhou, Z.R., Zhang, J., Li, H. and Yu, H.Y. (2003), "On the friction and wear behaviour of human tooth enamel and dentin", *Wear*, **255**(7-12), 967-974. [https://doi.org/10.1016/S0043-1648\(03\)00079-6](https://doi.org/10.1016/S0043-1648(03)00079-6).